GEORGIA INSTITUTE OF TECHNOLOGY OFFICE OF CONTRACT ADMINISTRATION

SPONSORED PROJECT TERMINATION/CLOSEOUT SHEET

Date December 3, 1987

Project No. E-21-J37 School/~~Lab~~ EE

Includes Subproject No.(s) N/A

Project Director(s) D. T. Paris GTRC / ~~GTL~~

Sponsor Naval Coastal Systems

Title Bubble Dissolution Project

Effective Completion Date: 9/30/87 (Performance) 9/30/87 (Reports)

Grant/Contract Closeout Actions Remaining:

- [ ] None
- [x] Final Invoice or Final Fiscal Report
- [x] Closing Documents
- [x] Final Report of Inventions Questionnaire sent to P.I.
- [x] Govt. Property Inventory & Related Certificate
- [ ] Classified Material Certificate
- [ ] Other _____

Continues Project No. _____ Continued by Project No. _____

COPIES TO:

Project Director
Research Administrative Network
Research Property Management
Accounting
Procurement/GTRI Supply Services
Research Security Services
Reports Coordinator (OCA) ✓
Legal Services

Library
GTRC
Research Communications (2)
Project File
Other Duane Hutchison
Angela DuBose
Rusty Embry

FORM OCA 69.285

08:25:18 OCA PAD INITIATION - PROJECT HEADER INFORMATION 10/09/87

Active

Project #: E-21-J37 Cost share #: Rev #: 0
Center # : R5962-BC7 Center shr #: OCA file #: 93
Work type : RES
Contract#: N61331-85-D-0025-0037 Mod #: Document : CONT
Prime #: Contract entity: GTRC

Subprojects ? : N
Main project #:

Project unit: EE Unit code: 02.010.118
Project director(s):
PARIS D T EE

Sponsor/division names: NAVY / NAVAL COASTAL SYS, FL
Sponsor/division codes: 103 / 001

Award period: 870824 to 870930 (performance) 870930 (reports)

Sponsor amount	New this change	Total to date
Contract value	15,053.00	15,053.00
Funded	15,053.00	15,053.00
Cost sharing amount		0.00

Does subcontracting plan apply ?: N

Title: BUBBLE DISSOLUTION PROJECT

PROJECT ADMINISTRATION DATA

OCA contact: E. Faith Gleason 894-4820

Sponsor technical contact

MR. EDWARD L. PIPKIN/CODE 4120
(904)234-4281
NAVAL COASTAL SYSTEMS CENTER
PANAMA CITY, FL 32407-5000

Sponsor issuing office

ALAN HOTTEL/CODE 0654
(904)234-4309
NAVAL COASTAL SYSTEMS CENTER
PANAMA CITY, FL 32407-5000

Security class (U,C,S,TS) : U ONR resident rep. is ACO (Y/N): Y
Defense priority rating : DO-S10 GOVT supplemental sheet
Equipment title vests with: Sponsor X GIT

Administrative comments -
INCLUDES SUBCONTRACT TO DALHOUSIE UNIVERSITY FOR $11,450.

E-21-J37

DALHOUSIE UNIVERSITY
HALIFAX, N.S.
B3H 4H6

November 9, 1987

OFFICE OF THE PRESIDENT

Dr. D.T. Paris
Electrical Engineering
Georgia Institute of Technology
Atlanta, Georgia
USA 30332-0250

Re: Subcontract No. E-21-J37-S1

Dear Dr. Paris:

I have enclosed a copy of the report "Small Bubble - Large Particle Interaction in Sea Water" prepared by Dr. Bruce D. Johnson under the terms of the above mentioned subcontract. Multiple copies of the report were submitted to Dr. Richard Detsch of the Naval Coastal System Center on September 30, 1987.

Thank you for your interest in research at Dalhousie University. If you have any questions about this subcontract do not hesitate to call me at 902-424-3859.

Sincerely,

Daniel Chase
Co-ordinator
Research Services

encl.

cc: Dr. B.D. Johnson
Mr. C. Stanford, Jr.
Ms. K. Knighton ✓

Scientific Report Summary	Effective Date : 24 August 1987
Order No. N61331-85-D-0025	Expiration Date : 30 Sept. 1987
Contract No. 7218-4120	Reporting period: 1-30 Sept. 1987

Georgia Tech Research Corp.
225 North Avenue N.W.
Atlanta, GA 30332

SMALL BUBBLE - LARGE PARTICLE INTERACTION IN SEA WATER

by:

B.D. Johnson
Department of Oceanography
Dalhousie University
Halifax, Nova Scotia CANADA
(902)424-3358

Submitted to:

R. Detsch
Naval Coastal Systems Center
Panama city, Florida

TABLE OF CONTENTS

LIST OF FIGURES

1.0 INTRODUCTION

The surface layer of the ocean is a dynamic system where complex physical and chemical phenomena occur, many of which are driven by, or otherwise associated with, the proximity of the air-water interface. An area of study attracting an increasing amount of attention in recent years concerns the various processes that are associated with air bubbles that have been injected into the water column by any of various means, the primary source being breaking waves. This is an important research field both because the presence of bubbles in the ocean significantly alters the physical properties of the water and because they provide loci for physico-chemical reactions by means of the immense air-water surface area they present.

Of particular concern to the present study is the interaction of bubbles with dissolved, colloidal and particulate matter in the ocean. The physical and chemical behaviour of particles and air bubbles in water is greatly modified by the presence of surface active components in the liquid phase. This can be true even when the concentration of such components is very low in the bulk phase.

Thus, while the study of bubbles and particles in the ocean must begin with a description of the basic fluid mechanics of the system, this must be extended to include the effects which change the surface properties of the bubbles and particles that, in turn, determine how they will interact with each other or with artificial particles introduced into the system.

2.0 OBJECTIVES

The primary goal of this work is to define an experimental protocol to investigate the behaviour of small bubbles and large particles in the aqueous environment. To this end we have provided in this document the following items:

- A literature review describing existing data that is of direct interest to the problem of large particle-small bubble attachment.

- A brief description of experiments performed in our laboratory that demonstrate our expertise in the field of bubble-particle interaction. These experiments deal primarily with techniques for the generation of bubbles, means of producing particles of known surface characteristics, and methods for the measurement of bubble-particle interaction.

- A proposal for a 2-year study that is designed to investigate the optimization of small bubble-large particle attachment in sea water.

3.0 LITERATURE REVIEW

3.1 Mechanisms of bubble-particle collision

Mechanisms of transport: Early treatments of particle collection by using bubbles, especially in mineral flotation, ignored the mechanics of bubble-particle collision as a factor. These studies are devoted entirely to improvements in surface chemistry, as it was widely believed that the process of flotation could be controlled through addition of the proper flotation reagents.

Since these early studies, the mechanisms of flotation have been described and a number of features of the process have been quantitatively modelled. The processes involved in flotation of particulate materials include:

- Collision of the bubble and particle and formation of a thin film;
- Decrease of the film thickness to the point of rupture;
- Film rupture with subsequent establishment of a stable three-phase system with characteristic wetting angles;
- Survival of the bubble-particle aggregate in a turbulent flow field.

A number of mechanisms for bubble particle collisions have been identified and include:

- Gravitational deposition
- Convective diffusion (in both laminar and turbulent regimes)
- Interception (laminar and turbulent)
- Inertial impaction (laminar and turbulent)

3.2 Dynamics of small bubbles in sea water

Bubbles injected into sea water potentially pass through three separate regimes of dynamics as their surfaces become increasingly covered with surface active dissolved colloidal and larger particulate materials. The surface of a recently-formed bubble is mobile, and unlike a rising solid sphere, the tangential fluid velocity at its interface does not go to zero. A torroidal flow is set up in the bubble interior (Levich 1962, Baccuber and Sanford 1974). In this state of having a mobile interface, the maximum rise velocity of the bubble is 3/2 greater than that predicted by Stoke's Law (which applies to bubbles of less than ca. 100 μm radius). The effect of surface mobility on mass transfer can be very great, in some cases providing considerable enhancement.

As the bubble rises it collects surface active material. This material, dissolved, colloidal, and particulate, is swept to the rear of the bubble, where it accumulates and establishes a surface tension gradient that opposes viscous drag on the bubble surface. As surface active material accumulates, the bubble interface becomes less mobile, and ultimately the bubble rises as a solid sphere, with its rise rate governed by Stoke's Law (for bubbles at $Re < 1$) or other resistance equations (at higher Reynolds numbers) for solid sphere motion. The efficiency of mass transfer of particulate material via convective diffusion or interception falls dramatically.

The third regime of bubble behaviour in sea water is characterized by bubbles that are stable to dissolution. These stable microbubbles act as cavitation nuclei and are responsible for the low tensile strength of all natural waters. Stable microbubble populations have been measured acoustically by Medwin (1977). In the absence of whitecaps or other known sources of bubbles, he found as many as 2×10^6 bubbles m^{-3} in the range of 17-350 μm radius to depths as great as 36 meters. Johnson and Cooke (1981) demonstrated that stable microbubbles as large as about 13 μm in diameter could be produced by bubble dissolution in filtered sea water samples (figure 3.1). While several mechanisms have been identified for stabilization of bubbles, the only one that appears to provide stability to

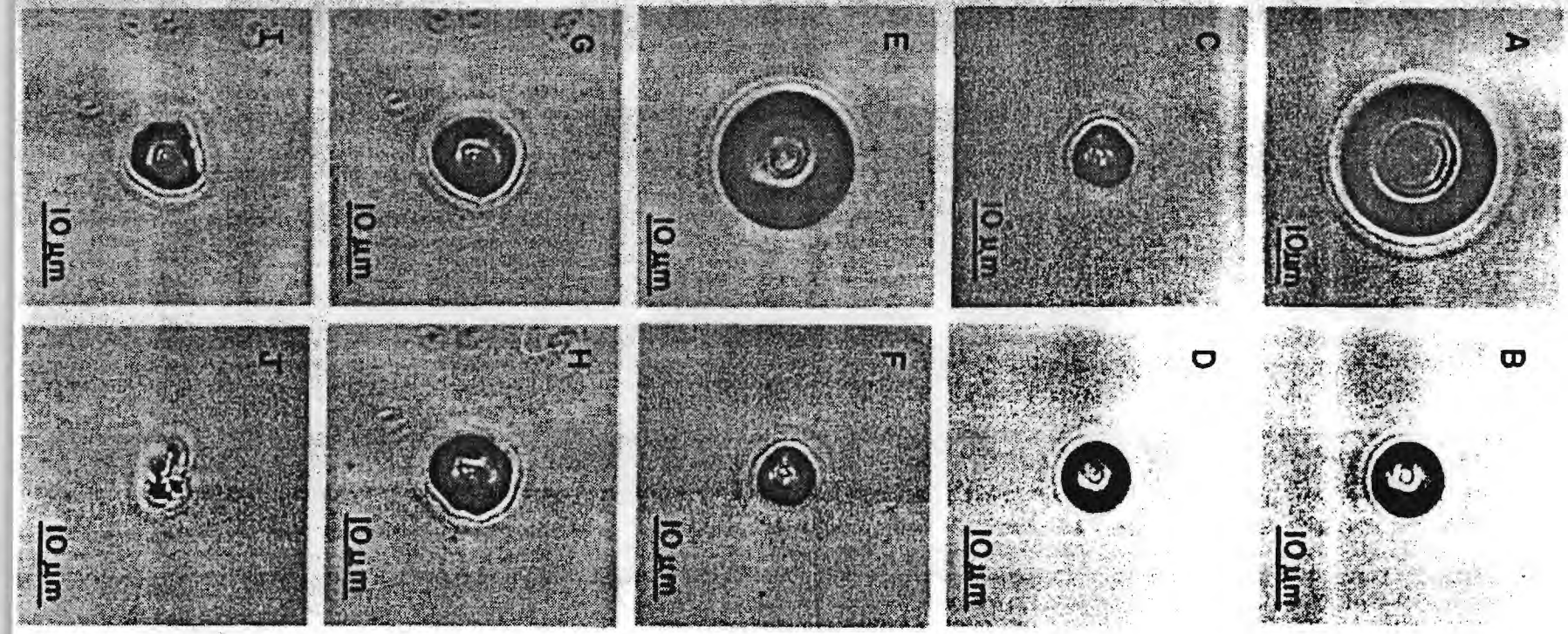

Figure 3.1 (A to C) Stable microbubble formed in sea water at 22°C, 1 atm.
(D to E) Expansion of microbubble under reduced pressure.
(F) Return to original size After pressure was restored.
(G) A second microbubble at atmospheric pressure,
(H) at 0.28 m water,
(I) at 0.69 m water,
(J) particle remaining After collapse of the bubble.

(After Johnson and Cooke, 1981)

sizes as great as those described by Medwin (1977) is stabilization by monolayers of adsorbed particles (Johnson and Wangersky, in press). Figures 3.2 and 3.3 show stable microbubbles that were produced in our laboratory using nonpolar particles.

While the result of such monolayer coverage may be reduced buoyancy (depending on the particle density), its behaviour in terms of particle scavenging must surely be dominated by the layer of adsorbed particulate material. The expected behaviour of such a particle-covered bubble in its interaction with larger particles would then be very different than that expected of bubbles with clean surfaces. This, because no thin film can form or rupture, nor can the stable three phase contact angle be established.

Such stable microbubbles must be considered here because bubbles as small as 5 μm have LaPlace pressures that cause very rapid bubble dissolution in air-saturated water. At 25°C, a bubble of 10 μm in radius dissolves in about 10 seconds. Thus for 5 μm bubbles to exist for significant periods of time, either very high gas supersaturations must be present (ca. 0.6 atmospheres), or bubble stabilization must be invoked. If these stable microbubbles are of near-neutral buoyancy, as suggested by Mulhearn (1981), then bubble rise cannot be used to enhance scavenging of large particles, but processes that promote collisions among neutrally buoyant particles must be considered instead. These include mechanisms that increase laminar and turbulent shear.

3.3 Modes of bubble-particle interaction

Were bubbles to collide with all particles in the cylindrical volume swept out by the bubble in rising, the collision efficiency would be by definition equal to unity. However, as the bubble rises, streamlines are deflected around the bubble, causing particles that follow these streamlines to likewise be deflected. Thus particles can reach the surface only when they follow streamlines that pass within $R_B + R_P$ of the bubble surface at $\theta = \pi/2$, where θ is the angle measured from the axis passing through the

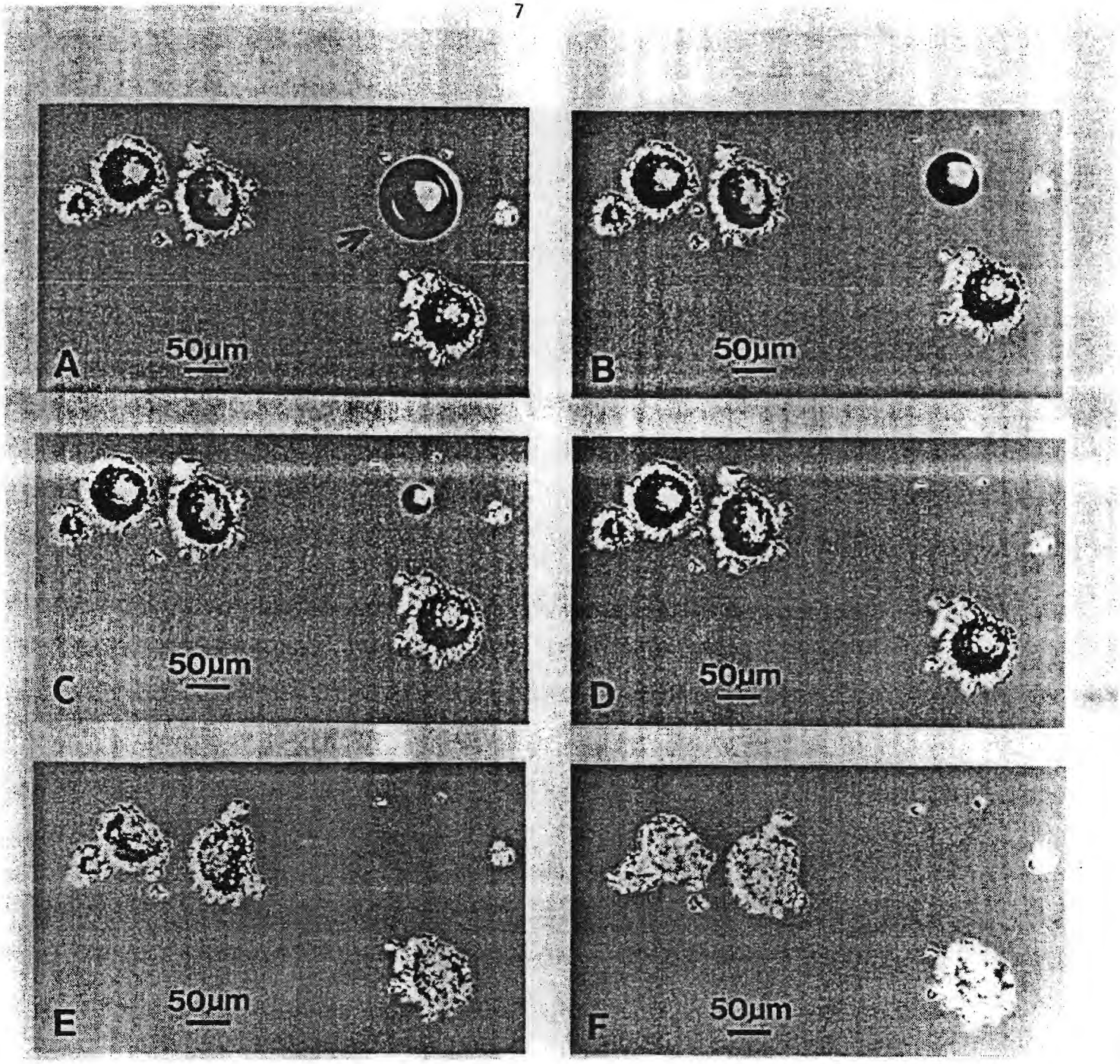

Figure 3.2 (A to D) Particle-stabilized microbubbles in distilled water at 22°C, 0.8 m water pressure remain unchanged while uncoated bubble dissolves.
(E to F) Addition of a pressure of 4 m water collapses microbubbles.

(After Johnson et al. in press)

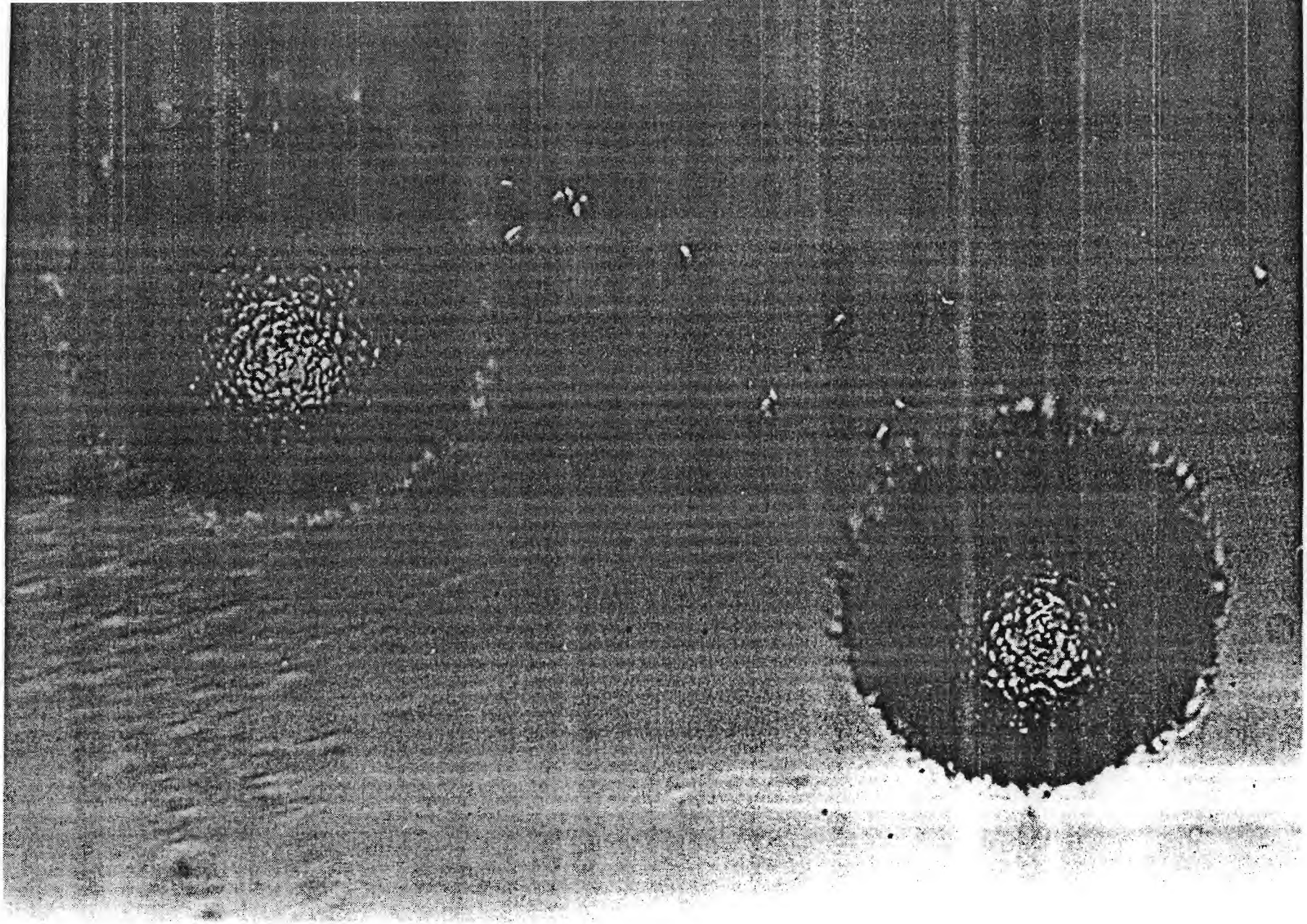

Figure 3.3 Particle-stabilized bubble showing particle surface coverage

bubble centre with $\theta = 0$ being at the point of incident flow (figure 3.4). R_M defines the distance from the bubble axis to the grazing streamlines at $x \approx \infty$, upstream of the bubble. Thus the collision efficiency between bubble and particle can be described by:

$$E_C = \frac{N\pi R_M^2}{N\pi R_B^2} = \left[\frac{R_M}{R_B}\right]^2 \qquad (3.1)$$

A relatively large literature exists in which bubble-particle trajectories are determined theoretically. However, there are few situations for which the equations of motion can be solved directly. More typically, approximate solutions are obtained or the equations are solved numerically.

Modes of bubble-particle interaction (convective diffusion): This process is important for particles for which Brownian motion is significant, i.e. particles of the order of less than a few μm in diameter. The parameters of importance are the Peclet number and the Reynolds number for which:

$$Pe = dV/D_f \qquad (3.2)$$

where d is the bubble diameter, V the rise velocity and D_f the diffusivity. For particles that undergo brownian motion, D_f can be expressed as the Einstein-Stokes equation:

$$D_f = \frac{KT}{6\pi\mu a} \qquad (3.3)$$

where K is Boltzman's constant, T absolute temperature, μ absolute viscosity and a the particle radius. The Reynolds number is given by:

$$Re = \frac{dVf}{\mu} \qquad (3.4)$$

in which f is the fluid density. Solutions for convective diffusion from a rigid sphere in creeping flow range from Sherwood number = 2 (pure diffusion from a motionless sphere in a stagnant fluid) to Sh proportional to $Pe^{1/3}$

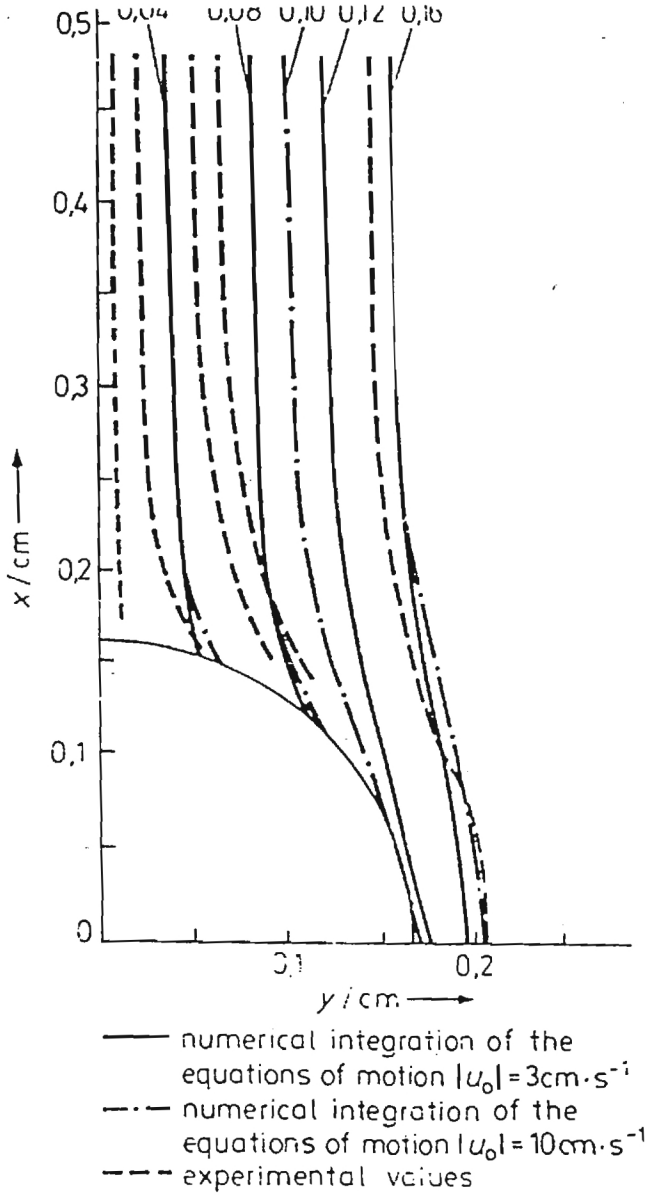

Figure 3.4 Flow streamlines around a rising bubble

(After Schulze, 1984)

when $Pe \approx \infty$. An approximate solution provided by Levich (1962) for $Pe \approx \infty$ is:

$$Sh = 0.991\ Pe^{1/3} \tag{3.5}$$

in which $Sh = KL/D_f$ where K is the mass transfer coefficient. For $Pe = 10^3$, Levich's (1962) solution gives a Sh about 10% too low; at lower Re the prediction of Sh is less accurate.

Acrivos and Goddard (1965) provided a first order correction to Levich's solution and obtained:

$$Sh = 0.991\ Pe^{1/3} + 0.92 \tag{3.6}$$

This solution lies within 3% of the numerical solution at Pe = 30.

For fluid spheres in creeping flow, the rate of particle transfer in convective diffusion depends upon the viscosity ratio μ_B/μ_W where B and W represent bubble and water. Levich (1962) offers the solution again at $Pe \approx \infty$ and here for $\mu_B/\mu_W = 0$ as,

$$Sh = 0.46\ Pe^{1/2} \tag{3.7}$$

Clift et al. (1978) provide a numerical solution which they approximate to within 6% at all Pe and also at $\mu_B/\mu_W = 0$ as:

$$Sh = 1 + (1 + 0.564\ Pe^{2/3})^{3/4} \tag{3.8}$$

Convective diffusion of particles at higher bubble Re requires solutions at Schmidt numbers ($Sc = \mu/fD_f$) that are very high.

An equation applicable to high Sc ($200 < Sc < 2000$) obtained by curve fitting a wide range of data for mass and heat transfer is given by Clift et al. (1978):

$$Sh = 1 + 0.724\ Re^{0.48}\ Sc^{1/3} \tag{3.9}$$

for $100 < Re < 2000$. For diffusivities as low as those predicted for colloidal particulate material, Sc are much higher than are typically treated in the literature.

Convective diffusion to a rising bubble ($\mu_B/\mu_W \approx 0$) at $Re > 70$ is presented by Clift et al. (1978) as:

$$Sh = \frac{2}{\sqrt{\pi}} \left[1 - \frac{2.89}{Re^{\frac{1}{2}}} \right]^{1/2} Pe^{\frac{1}{2}} \qquad (3.10)$$

a result that agrees with numerical solutions to within about 7%.

Modes of bubble-particle interaction (interception): For transfer of particles with density contrast $\delta f \approx 0$ and sizes greater than about 10^{-5} cm, interception exceeds convective diffusion in importance for mass transfer to bubbles with a fluid interface rising in water. A solution for the efficiency of interaction of particles with bubbles having mobile interfaces in the Stoke's Law regime ($Re << 1$, e.g. Johnson 1981) is:

$$E = a/A \qquad (3.11)$$

This result predicts a very much greater efficiency for collection by a bubble with a fluid interface than is predicted for bubbles with an immobile interface. A difference of several orders of magnitude in collection efficiency is predicted. Weber et al. (1983) offer an equation for particle interception by a solid sphere obtained by approximating numerical solutions. For spherical particles colliding with a rigid sphere at $Re < 300$, he gives:

$$E = \frac{3}{2} \left[1 + \frac{3/16\ Re}{1 + 0.249\ Re^{0.56}} \right] \left[\frac{a}{A} \right]^2 \qquad (3.12)$$

in which a is particle radius and A the bubble radius.

For interception by a fluid sphere (applicable to collection of spherical particles) Weber et al. (1983) give for all Re:

$$E_i = \left[1 + \frac{2}{1 + (37/Re)^{0.85}} \right] \left[\frac{a}{A} \right] \qquad (3.13)$$

This reduces to eq. 3.11 at low Re. From both eqs. 3.12 and 3.13, a strong dependence on the ratio of particle size to bubble size is evident, with collision efficiency increasing with increasing ratio.

None of the above equations were developed for the case of small bubbles interacting with large particles. The equations for interception could conceivably be used with the two radii (bubble and particle) reversed, but only for the case in which the particle velocity greatly exceeds the bubble rise rate.

Modes of bubble-particle interaction (inertial forces): A number of approximate equations have appeared in the literature for describing collision efficiencies for bubbles and particles when the latter experience significant inertial forces. Langmuir (1942) gives,

$$E = \frac{K_L^2}{(K_L + 1/5)^2} \qquad (3.14)$$

where

$$K_L = \frac{2R_p^2 \delta f U_0}{9\mu R_B} \qquad (3.15)$$

and U_0 is the fluid velocity at a large distance from the bubble.

Sutherland (1948) derived,

$$E = \frac{R_M^2}{R_B^2} \cosh^2 \left[\frac{3U_\infty \tau_{SL}}{4R_B} \right] \qquad (3.16)$$

where

$$R_M = \sqrt{3}\, R_p\, R_B \left[\cosh \left[\frac{3\, U_{Rel}\, \tau_{SL}}{4\, R_B} \right] \right]^{-1} \qquad (3.17)$$

in which τ_{SL} is the sliding time and U_{rel} is the relative velocity between the bubble and particle. Particle trajectories that reach the bubble surface at an angle less than some critical angle ϕ_c (or ϕ_{lim}) are likely to attach. Those that follow trajectories that interact with the bubble at angles greater than ϕ_c merely slide over the bubble surface. The sliding time is defined as the interval when $\phi \approx 90°$.

The collision efficiency according to Fuks (1955) is simply,

$$E = \frac{3R_p}{R_B} \qquad (3.18)$$

for all $\phi < 90°$ while Anfruns and Kitchener (1977) give,

$$E = \frac{(1 + R_p/R_B)^2}{1 + Gp} \left[Gp + \frac{2\Phi}{(1 + R_p/R_B)^2} \right] \qquad (3.19)$$

for St = 0.1 in which St is the Stokes number, Φ the stream function at the bubble equator at a distance R_p from the bubble surface and G_p the dimensionless gravity parameter.

Features predicted by the inertial collision equations are (Schulze 1975):

- For particles with St > 1, the collision efficiency depends primarily on drag and inertial forces. Since St is proportional to Re and Re is a function of U_B, the bubble rise velocity, and R_B and since U_B in the Stokes regime is approximately proportional to R_B^2, then St increases with increasing bubble radius. Thus the collision efficiency increases with increasing bubble radius.

- For St < 0.1 the collision efficiency is nearly independent of St, but dependent on G_p. G_p decreases with increasing bubble size because G_p varies inversely as the bubble rise velocity. The collision efficiency can be enhanced only by diminishing the bubble size.

- In flotation systems E can never be zero, since G_p cannot be zero.

- For a given St, the collision efficiency is higher with potential flow around the bubble than with Stokes flow.

- Very fine particles follow the streamlines and can only be captured if these streamlines intersect the bubble.

- Large particles can only touch the bubble in the region $0<\phi_t<90°$ with the upper limiting velocity being the smaller the larger is the particle limiting velocity.

3.4 Microflotation studies

While microflotation typically treats the flotation of small and colloid-size particles, the relevance of this literature for collisions of small bubbles with large particles will become apparent during this synthesis.

The sizes of bubbles and particles have proven to be important factors in the rate of flotation. Morris (1950) found the rate of flotation to be proportional to $\ln(d_p)$, where d_p is the particle diameter. Gaudin (1957) found that the rate of flotation was independent of d_p in the particle size range of 1-4 μm, and directly proportional to d_p from 4 to 20 μm. Collins and Jameson (1976) reported that in flotation of polystyrene particles, the rate varied as $d_p^{1.5}$. Similarly, Reay and Ratcliffe (1973) found a somewhat higher dependence (d_p^2) for flotation of glass spheres above 1 μm in diameter. They concluded that a 1 μm particle size represented a minimum efficiency for flotation. Tomlinson and Fleming (1963) have reported that flotation rate is proportional to d_p^2 for easily floated minerals and to d_p for less easily floated minerals.

These results almost universally suggest that flotation efficiency increases with increasing particle size above sizes of about 1 μm. This conclusion is supported by results of theoretical treatments of interception of particles by rising bubbles. For example, Johnson and Cooke (1981) found that collision efficiency by interception (Re<1) increased as d_p to the first power for bubbles with mobile interfaces and showed a somewhat greater dependence on d_p for bubbles with immobile interfaces. A minimum interception efficiency for bubbles with mobile interfaces was predicted at about 0.2 μm particle size. This minimum occurs at the intersection of the convective diffusion and interception particle size-collision efficiency curves (figure 3.5).

In a number of microflotation studies, flotation was benefitted by floculation of the small and colloid size particles, again demonstrating improved efficiency with larger size particles. Rubin and Erickson (1971) found an enhanced rate of removal of illite with hetero-floculation with alum. Similarly, Mangravite et al. (1972) enhanced the flotation rate of colloidal silica through heterocoagulation with aluminum hydroxide particles. Devivo and Karger (1970) found improved flotation performance for floculated kaolin and montmorillonite with bubbles of 0.2 mm diameter. However, they also found that floculation rate was reduced in the presence of flocs when 1-2 mm bubbles were employed. They concluded that small bubble flotation was enhanced because more than one small bubble could

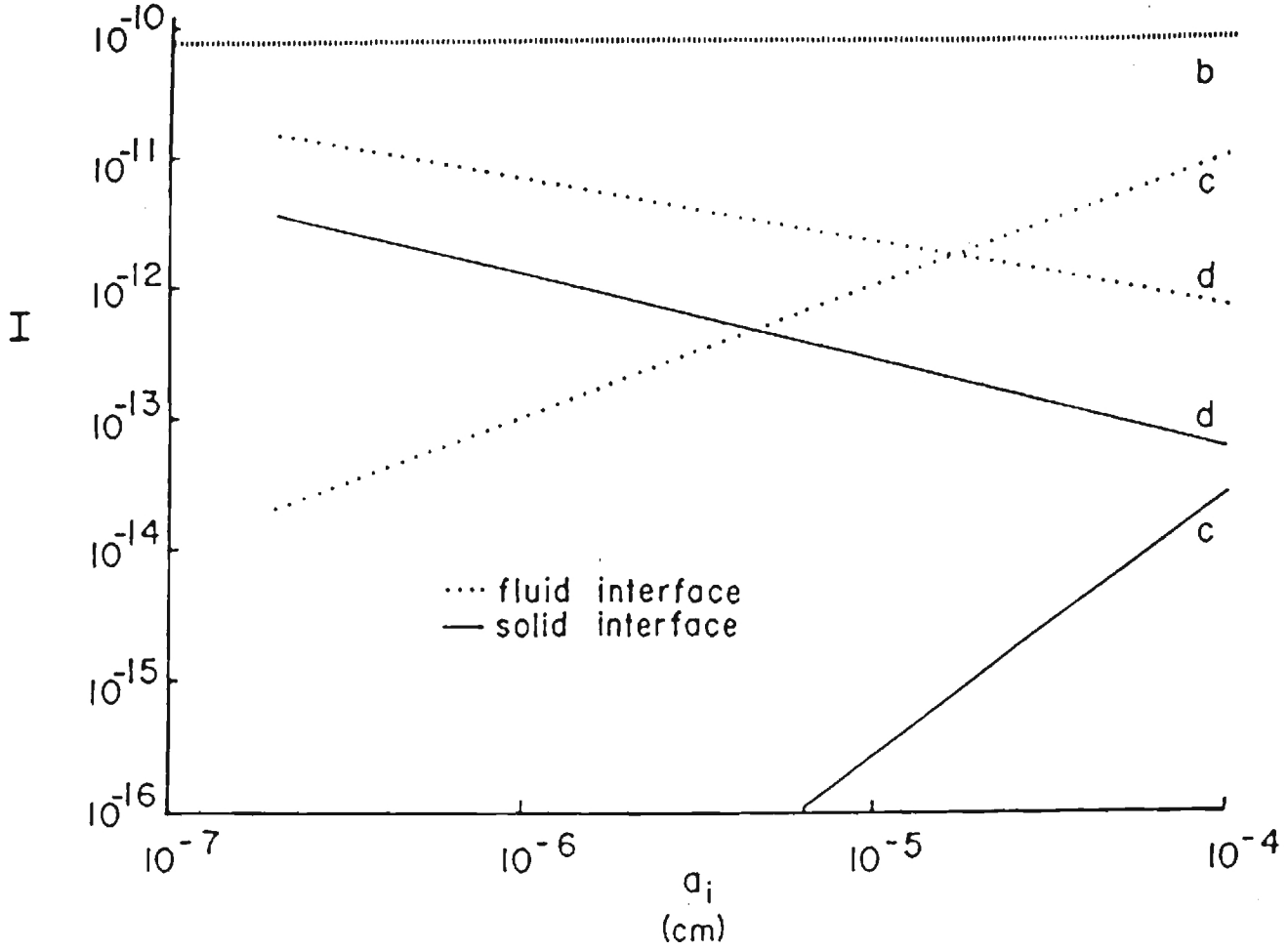

Figure 3.5 Collection efficiency by interception and convective diffusion

(After Johnson 1982)

attach to a given aggregate. In general, floculation which produces increased particle size improves flotation, however, the process is affected by factors that are not a concern in discrete particle flotation; for example, aggregate break-up by larger bubbles or in turbulence and small bubble entrapment in the floc matrix.

Small bubble size thus appears to be favoured in flotation of flocs. Few studies of the flotation of discrete particles have examined the effect of bubble size, and indeed, many do not even report bubble size. Among those that have examined bubble size, the results are somewhat difficult to assess. Reay and Ratcliffe (1975) suggest that flotation rate for glass spheres is independent of bubble size to sizes as great as 100 μm. Johnson et al (1986) observed that the rate of surface coagulation improved with larger bubble size. Still others have suggested that smaller bubble size increases flotation rate. The confusion here is probably due to measurements that include other factors such as bubble aggregate break up. The measured rate of flotation is then only a net rate.

3.5 Particle trajectories

Theoretical treatments of bubble-particle interaction have been tested most effectively using stroboscopic methods (Flint and Howarth 1971). When illuminating a cross-section of a bubble with a narrowly collimated sheet of light from a strobe, photographs taken normal to the plane of light reveal the trajectories of particles approaching in a fluid stream. Particle-bubble interactions can be recorded, and precise timing of events can be determined from the strobe interval. This kind of experiment has permitted the visualization of a number of details of the bubble-particle interaction process. For example, particle trajectories, grazing streamline identification, collision efficiency and sliding time have all been estimated using this technique.

Particles that approach a bubble follow trajectories that result in one of three kinds of behaviour:

- collision and elastic recoil
- particle attachment
- particle sliding

Elastic recoil occurs either when the particle collides with the bubble surface for a time too short for the intervening thin film to rupture or when, even if the film ruptures, the elastic rebound of the particle occurs with a force that exceeds the adhesive force of the particle on the bubble. In experiments, particle rebound has been observed for both small and large touching angles (angle from the point of fluid incidence). In the former case, contact time is too short for film rupture, while in the latter, the contact time is sufficiently great, but the energy of contact is insufficient for film rupture. Intermediate contact angles appear to provide the best condition for attachment.

The form of bubble-particle interaction known as sliding occurs when particles follow trajectories that interact with the bubble surface at angles greater than a specific limiting angle. Trajectories that touch the bubble at angles less than this limiting angle typically define the range that result in collisions. Experimental results suggest that this limiting angle is about 30° (Schulze 1984). The stroboscopic experiments also show that the collision efficiencies predicted by the equations of Langmuir (1942), Fuks (1955) and Sutherland (1948) are reasonable.

3.6 Thin liquid films between particles and bubbles

Interparticle forces operate when the film between a bubble and particle is of the order of 100 to 200 nm thick. These forces presumably dominate the interaction at these separation distances, and can enhance the rate of film thinning or even prevent closer approach. The free energy of the thin film between the bubble and particle differs from the free energy of the bulk liquid phase. This difference in free energy is accompanied by a pressure difference in the film - the disjoining pressure π. When π is less than zero repulsive forces dominate, when greater, attractive forces prevail.

There are three contributors to the disjoining pressure:

- ion electrostatic components
- electrodynamic components
- structural components

The electrostatic forces arise from interaction of ion double layers. These forces tend to produce positive disjoining pressures and can be predicted from DLVO theory.

The electrodynamic component is the result of London-VanderWaals forces and have typically been treated by the microscopic theory of Hamaker. However, the accuracy of this method has been questioned. An approach found to be more reliable is the macroscopic theory using spectroscopic data (Ninham and Parsegian 1970).

Structural forces are the result of interaction of structured water at the gas-water interface or of elastic repulsive forces of adsorbed surfactant layers on bubble and particle surfaces. This structural interference is also known as steric hinderance.

A number of techniques have been used to measure properties of thin films, and especially film thickness between particles and bubbles. Among these methods are interferometry, light scattering and ellipsometry. Measurements that are also important include the electrophoretic behaviour of bubbles and particles. These parameters can be determined from electrophoretic mobilities of particles and small bubbles in standard cells. For larger bubbles, the cells are rotated to keep the bubble suspended. The value of particle and bubble electrokinetic potential measurements for prediction of attachment was demonstrated by Fukui and Yiu (1980). They found that when the product of the bubble and particle zeta potentials was greater than zero, the particle collection efficiency was low. When the zeta potential product was negative attachment efficiencies were high.

This result is consistent with the theory that predicts that opposite charges on bubble and particle produce unstable films. If the charges are of the same sign, electrostatic repulsive forces make the thin wetting film stable. The film can be made unstable only by reversing the charge on one of the surfaces, usually the particle, by adding a surfactant, i.e., a collector. However, numerous experiments in flotation describe the decline in performance of flotation beyond a critical concentration of collector. This decline may be due to exceeding the critical micelle concentration of the collector.

Thin film rupture: When unstable films reach a certain thickness, h_{crit}, they rupture spontaneously. Whether a particle will adhere to a bubble is largely dependent on whether the thin film ruptures during the bubble-particle contact time. Spontaneous film rupture does not occur if repulsive forces are operative. The last stipulation can be expressed as $\Sigma\pi<0$, i.e. the sum of all disjoining pressures are less than zero.

Several other factors appear to be important in the rupture process. These include the area of contact with attendant time required for film draining, and particle roughness. Particles that are irregular in shape, particularly those with sharp peaked surfaces, puncture the film at a number of places and enhance the rate of film draining. When the thin film ruptures, a three phase line of contact (TPC) is established. The rate of spread of the TPC must be sufficiently great to permit a force of attachment to counter hydrodynamic forces.

For non-spherical particles, additional rotational instabilities must be considered. However, nonspherical particles, expressed in terms of equivalent spherical size, offer a larger maximum floatable volume. Anfruns and Kitchener (1977) found a significant rise in collection efficiency of irregularly shaped particles as compared to spherical particles. Flotation of the irregular-shaped particles approached theoretical rates. This increased efficiency may be due to both improved adhesion and to enhanced film rupture rates.

3.7 Effect of sea water on bubble-particle interactions

Bubble-particle interactions in sea water can be expected to be affected by the composition of the medium. Surface sea water contains of the order of 0.1 mg l^{-1} particulate organic carbon and 1 mg l^{-1} dissolved organic matter. Much of this dissolved and particulate material is surface active, containing lipids, carbohydrates, proteins and largely uncharacterized macromolecular substances (Gershey 1983). Wallace and Duce (1975) found from floatation experiments that 50% of the particulate organic carbon in their sea water samples was flotable in only 15 minutes of vigourous bubbling. Both the inorganic and organic substances in sea water have a profound influence on the surface chemical and electrokinetic properties of particles and bubbles as well.

The high ionic strength of sea water causes electrical double layers to be compressed, effectivly reducing the extent of electrostatic forces. Other contributions to the disjoining pressure must then dominate. In particular, the structural forces must be considered.

Studies by Niehoff and Loeb (1972) and Hunter (1980) have shown that surfaces in sea water acquire an adsorbed layer of organic matter that subsequently dominates the surface chemistry of, for example, particulate material. Several features of their results are likely to be important here. Hunter (1980) found that regardless of the surface character of the particles before introduction to sea water, i.e. whether they had hydrophilic or hydrophobic character, they invariably acquired an organic surface film. This surface film always produced a change in electrophoretic mobility indicative of a narrow range of slightly negative surface charge.

While we know of no studies describing electrokinetic behaviour of bubbles in sea water, it is likely that adsorption of surface active materials modifies bubble surface character. Adsorbed colloidal and particulate materials that are forced into close packing because of bubble dissolution (figure 3.6) must dominate the surface properties of the bubble. A determination of the magnitude and kinetics of these background effects must be included in studies of bubble-particle interactions in sea water.

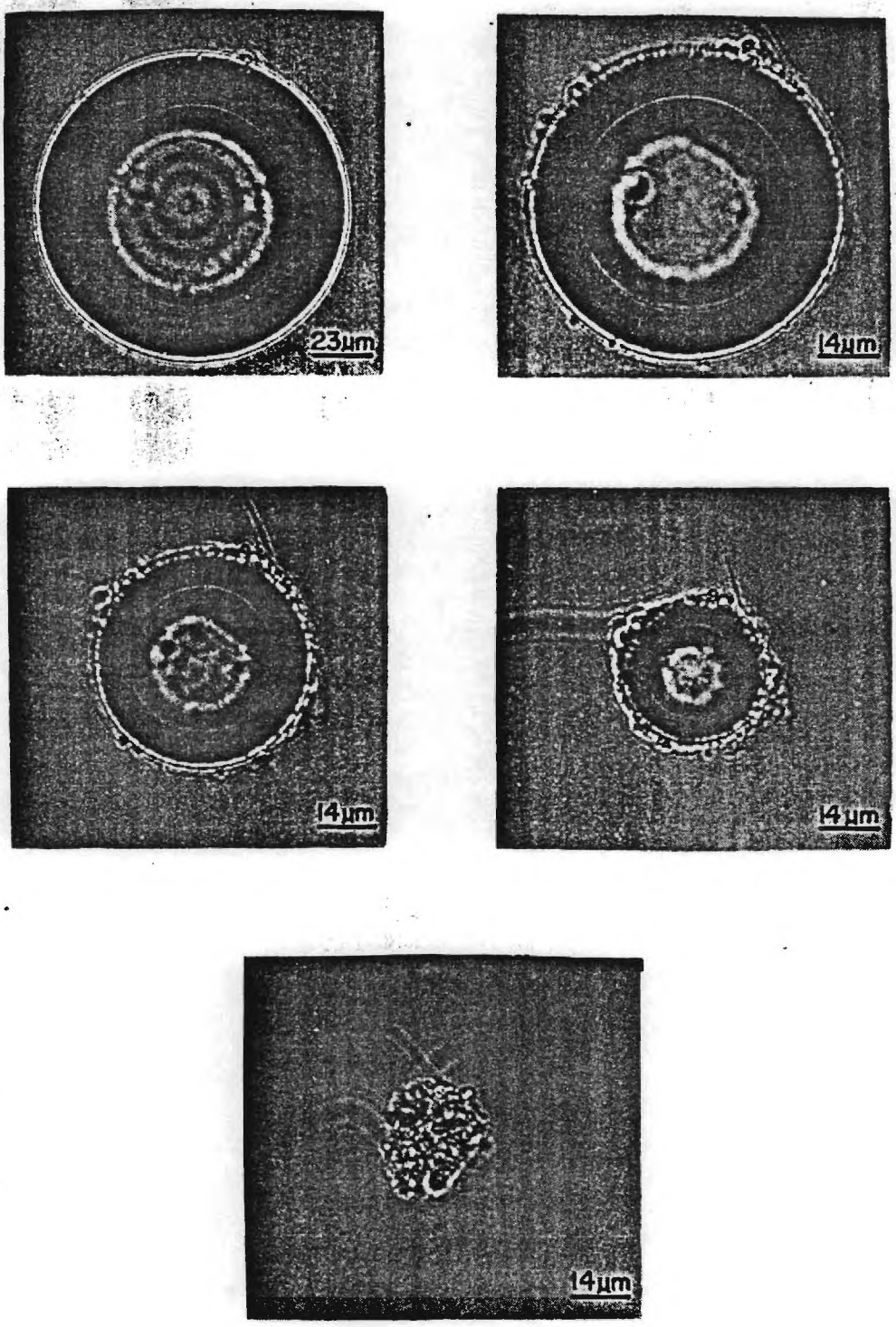

Figure 3.6 Progressive dissolution of a bubble that had been aged for 20 sec in unfiltered sea water.

3.8 Surface property modifiers

As mentioned in sections 3.1 and 3.6, bubble-particle attachment is strongly influenced by the stability of the thin liquid film between the bubble and particle. Several workers have investigated the use of tensides as a means to destablilize the thin films and thus promote particle attachement (e.g. Blake and Kitchener 1972, Schulze 1975).

The main mode of action of the compounds used is to reverse the surface charge of the interfaces which thus gives rise to electrostatic forces of interaction. Specifically, the effect of cation active tensides, such as long-chain alkyl amines, long chain fatty acids (e.g. arachic and stearic acids) deposited as Langmuir-Blodgett films, and silanol groups have been tested with regard to thier ability to destabilize thin films between bubbles and particles (Clint and Walker 1974).

The results of these experiments showed that even very low concentrations of tenside can lead to film instability. Concentrations of dodecylamine hydrochloride in the range of 10^{-7} molar produced significant film instability on silica surfaces, indicating that instability is induced with only a small degree of adsorption layer coverage (Schulze 1984). A study of similar amines of carbon chain lengths ranging from C_8 to C_{12} revealed that the the concentration of C_{12} amine necessary to produce the same effect as the C_8 amine was about an order of magnitude less. Finally, high concentrations of the tenside leads to a reversal of the effect, presumably due to the low solubility of the agent with attendent formation of micelles, which in turn interfere with bubble-particle attachment.

It is of particular interest in the context of this study to note that the very low concentrations that are required to produce an effect would render feasible the use of such a material as a field treating agent.

4.0 RESULTS OF PRELIMINARY EXPERIMENTS

4.1 Bubble generation

To enable one to conduct experiments into bubble-particle interaction it is necessary to have available convenient and effective means to generate many or few bubbles of a specified size or size range. This is by no means a trivial problem and in the past, a wide variety of means have been used for bubble production in the laboratory. We describe here the techniques that we have used in our laboratory both for the production of single bubbles of a specified size and for the production of large populations of bubbles with a narrowly defined size range.

Shear-type bubble generators: We have previously described two devices that produce large populations of small (15-100 μm) air bubbles in water with predictable size distributions (Johnson et al. 1982a, 1982b). Both employ a porous surface to initially form bubbles which are then subjected to a shear fields that detach bubbles of a predictable size range. Gas bubbles formed at an orifice submerged in a liquid grow until the surface tension force holding them to the solid surface is exceeded by a removal force. The latter force can be caused by the buoyancy of the bubble, inertial forces caused by the displacement of the liquid or drag forces arising from the presence of an external shear field.

Two configurations of shear bubble generators have been developed and tested in our laboratory, namely, the frit and disc generator and the cylinder and sleeve generator.

The cylindrical frit and sleeve bubble generator, is theoretically capable of producing large numbers of bubbles which should have size distributions that are virtually monodisperse. Presented here is a theoretical model that predicts the size distribution expected from such a device. We also report on the performance of this bubble generator and compare the bubble populations produced with the predictions of the model.

The frit and sleeve bubble generator (figure 4.1b) is a device which constrains fluid flow along a narrow channel at the surface of a cylindrical frit, thus providing a uniform fluid boundary layer. By adjustment of the volume flow rate of liquid, the drag force on a bubble emerging from the frit can be controlled and this in turn determines the size of the bubble when the attachment force is exceeded.

The following assumptions were used in the development of a model to predict bubble size as a function of fluid flow rate, channel width, and frit pore size:

- The flow over the frit surface is laminar and fully developed over the length of the cylindrical surface;
- Bubbles emerging from the frit pores experience significant force only from drag due to the fluid flow;
- The gas to water flow rate ratio is sufficiently small so that their is no significant bubble-bubble interaction and the properties of the fluid remain unchanged;
- Fluid flow streamlines are not affected by interactions with bubbles upstream or affected by surface roughness of the frit.

Given the above conditions, separation of the bubble at the frit occurs when the drag force caused by the fluid flow exceeds the attachment force due to surface tension, $\pi D\Gamma$:

$$C_D \frac{\rho U_o^2 A_p}{2} = \pi D\Gamma \qquad (4.1)$$

where ρ is the fluid density, U_o is the fluid velocity, A_p is the projected bubble area, Γ is the gas-water surface tension, and D is the pore diameter of the frit. The effective drag coefficient is C_D.

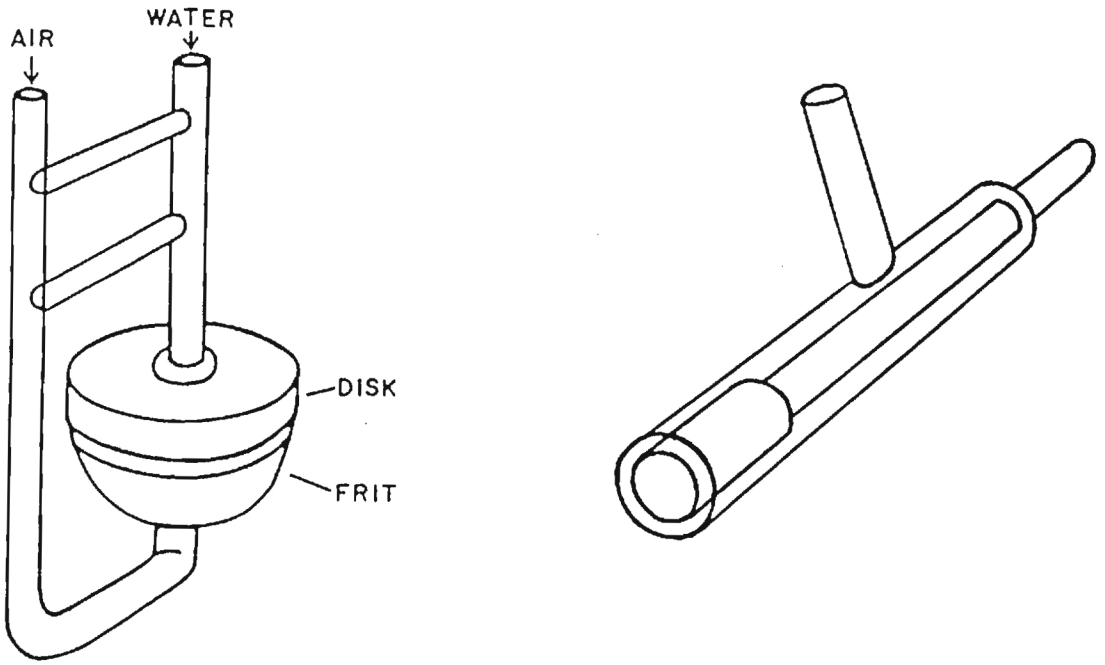

Figure 4.1 a) Frit and disc bubble generator
b) Cylinder and sleeve bubble generator

Since the flow is developed, there exists a velocity profile across the channel that varies from zero at the walls to a maximum at S/2 where S is the channel width. If the channel width is small compared to the radius of curvature, fully developed fluid flow in a cylindrical annular channel has a parabolic velocity profile as given for flow between stationary parallel boundaries:

$$U = \frac{G}{2\mu}(Sy - y^2) \qquad \text{or} \qquad U = \frac{S^2G}{8\mu}\left[\frac{4y}{S} - \frac{4y^2}{S^2}\right] \tag{4.2}$$

where G is the pressure gradient, μ the dynamic viscosity and y the distance from one wall, in the present case, the surface of the frit. The average velocity is obtained by integrating U over S and dividing by S giving:

$$U_{avg} = S^2G/12\mu \tag{4.3}$$

The volume flow rate is related to the average flow rate of fluid through the channel as follows:

$$U_{vol} = U_{avg}\,(\pi r_1^2 - \pi r_2^2) \tag{4.4}$$

where r_1 and r_2 are the radii of the sleeve and frit respectively. By rearrangement and substitution of (4.2-4.4) the local velocity as a function of volume flow rate can be written as:

$$U = \frac{3}{2\pi(r_1^2 - r_2^2)}\,U_{vol}\left[\frac{4y}{S} - \frac{4y^2}{S^2}\right] \tag{4.5}$$

The hydrodynamic drag (4.1) experienced by an emerging bubble is proportional to the quantity obtained by integrating the square of the local velocity over the projected area, A_p, of the bubble. This result is obtained by conversion of (4.5) to cylindrical coordinates followed by integration:

$$U_o^2 A_p = \frac{U^2_{vol}\, R^4}{\pi (r_1-r_2)^2 (r_1^2-r_2^2)^2} \left[\frac{45}{2} - \frac{63}{(r_1-r_2)} + \frac{189\, R^2}{4(r_1-r_2)^2} \right] \quad (4.6)$$

Substitution into (4.1) yields:

$$\pi D\Gamma = \frac{C_D f\, U^2_{vol}\, R^4}{\pi (r_1-r_2)^2 (r_1^2-r_2^2)^2} \left[\frac{45}{2} - \frac{63}{(r_1-r_2)} + \frac{189\, R^2}{4(r_1-r_2)^2} \right] \quad (4.7)$$

where R is the bubble radius. Bubble separation occurs when the drag force at a given radius exceeds the surface tension force.

The distribution of bubble sizes produced by one version of a cylinder and sleeve bubble generator is shown in figure 4.2a. The size distribution is quite tight but not monodisperse, this as a result of the properties of the glass frit used, i.e. surface roughness and pore size distribution. With further refinements, the distribution could be made significantly narrower. We are currently testing a model which uses a more highly polished stainless steel frit and sleeve. By adjustment of the water flow rate, the size of the bubbles in the distribution may be uniformly varied.

The frit and disc generator operates on much the same principles as outlined above but differs significantly in several respects. In construction, a glass disc is kept in position above the surface of a circular frit of the same diameter by a glass tube passing through a hole in the disc center (figure 4.1a). Water is pumped through the tube, separates the frit and disc and flows radially outward along the frit surface forming the shear field. Because the water velocity varies radially along the frit surface, the drag experienced by an emerging bubble and thus the size at separation is a function of position on the frit surface. Unlike, the cylinder and sleeve generator, then, a monodisperse population is not theoretically possible.

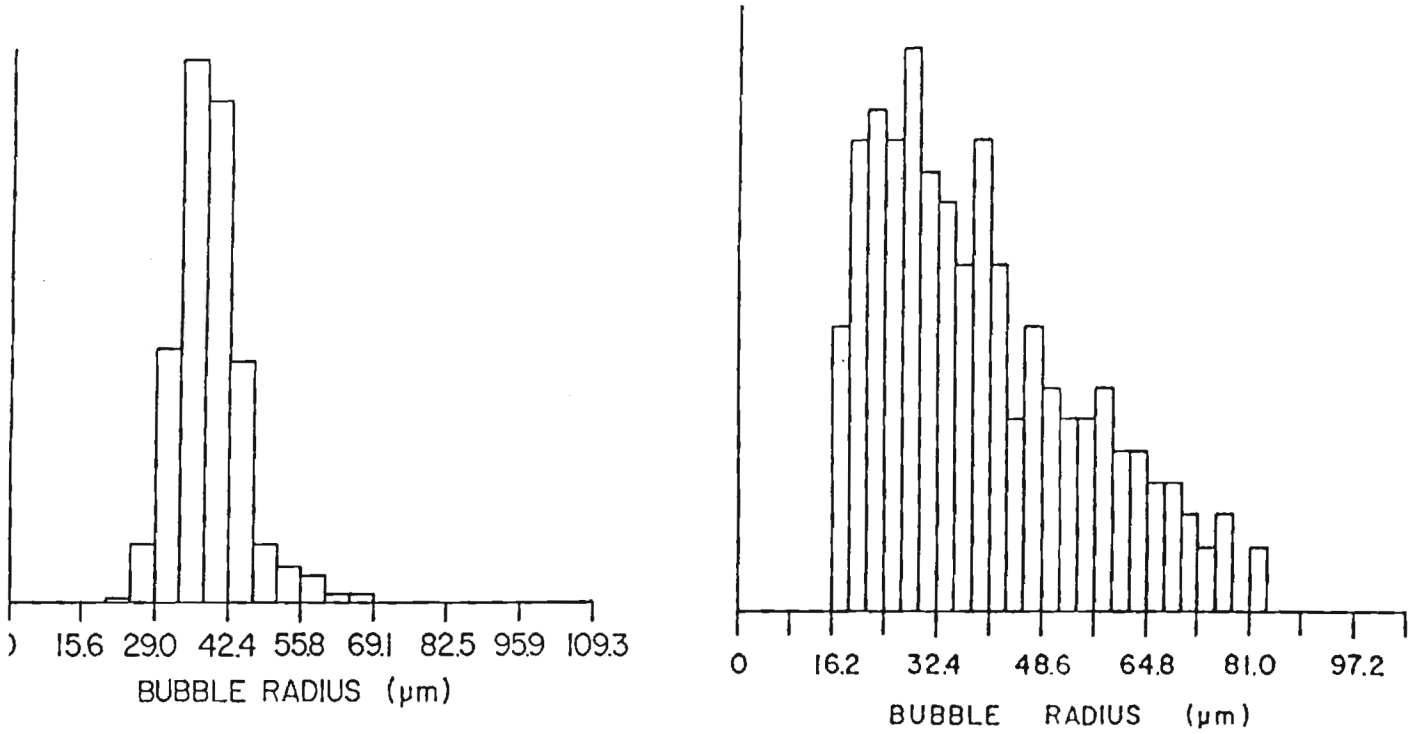

Figure 4.2 a) Bubble distribution from the cylinder and sleeve generator
b) Bubble distribution from the frit and disc generator

A model has been developed to predict the size distribution of bubbles produced by this device and was based on the same principles outlined above for the cylinder and sleeve generator. Taking into account the effect of the differences in physical construction between the two devices, the following results are obtained.

Analogous to (4.7), bubble separation occurs when the following conditions are met,

$$\pi D\Gamma = \frac{C_D f\, U^2_{vol}\, R^4}{4L^2 S^4 \pi} \left[\frac{45}{2} - \frac{63\, R}{S} + \frac{189\, R^2}{4\, S^2} \right] \qquad (4.8)$$

where S is the channel width, here the separation of frit and disc and L is the radial position of bubble measured from the centre of the frit. The number of bubbles, N, of a given size formed by the device is given the result of integrating the water and air flow rates over the surface of the frit,

$$N = \frac{3C_D f U^2_{vol} W}{8L^2_w S^4 \pi^3} \left[45\, R - \frac{315\, R^2}{4\, S} + \frac{567\, R^3}{12\, S^2} \right]_{R_1}^{R_2} \qquad (4.9)$$

where W is the total gas flow rate and L_w the radius of the frit.

Figure 4.2b shows a typical bubble distribution that can be obtained with this device. Comparison with figure 4.2a shows that the frit and disc generator produces a distribution which is much broader than that obtained from the cylinder and sleeve generator. The peak of the distribution may be moved up or down the size axis by altering the flowrate of water through the device.

4.2 Bubble/microlayer "filter"

A major requirement for conducting studies on particle flotation is the ability to determine numbers of particles transported per bubble, or in terms of the mass transfer coefficient K, the number of particles floated as a function of concentration, bubble surface area and time. Some of the methods that have been described in the literature include:

- Photographs of bubble-particle aggregates;

- Trapping of the floated particles in a surface foam fraction, followed by chemical or optical determinations of particle concentration in the original sample. In some studies the foam is collected, collapsed and particle yield determined.

Both of these methods suffer from limitations. Photographic determinations are often difficult to quantify because of inadequate resolution, depth of field limitations, or obscuration of particles on portions of the bubbles surface. Quantification of small bubble attachment to large particles is particularly difficult using photography because of particle opacity. Usually photographs are used to interpret other data, i.e., to determine state of floculation of particles, or whether more than one bubble is attached to a particle or particle aggregate.

Processes that require trapping the particles in foam have been used effectively, although particles can return to the suspension as foam collapses or is broken up in near-surface turbulence.

To determine the rate of mass transfer, the steady state concentration of bubbles in the sample is necessary information. This can be determined from the bubble size and the gas hold up. The latter information is particularly difficult to determine in conventional bubbling systems.

We have developed several techniques that permit determination of both the rate of bubble flotation in batch experiments and the particle load transported by individual bubbles. The first of these methods is one that we call microlayer filtration, and involves passing bubbles through a porous, non-polar membrane. The gas bubble wets the surface of the membrane and rapidly passes through the pores, depositing the floated material on the membrane surface. When the membrane defines the upper surface of the flotation chamber, a head of water in a sidearm can be used to maintain the water interface against the membrane. The LaPlace pressure prevents water passage through the pores in the membrane, and the gas holdup can be determined from the difference in water level in the sidearm before and during bubbling. While we are still improving this method, we feel that there are clear advantages in its use for studying particle flotation.

Examination of particles transported by individual bubbles can be achieved by microlayer filtration, as previously described, or by methods that we have developed for isolating individual bubble-particle aggregates. With this method, a single bubble-particle aggregate is isolated using a segregation tube filled with water and deposited either in a cell where it can be examined directly, or in a droplet of water where it can be allowed to dissolve. Evaporation of the water droplet then permits study of the material transported by the bubble.

While the details of both of these methods are somewhat more complicated than is described here, we have found them very effective in our studies of particle flotation.

5.0 PROPOSED EXPERIMENTS

5.1 Introduction

Sea water is a unique medium for conducting studies on bubble-particle attachment. The ionic strength of sea water is high, causing compression of electrical double layers and reducing the range of electrostatic interactions. As was discussed in the literature review, some fraction of the dissolved or colloidal organic matter in sea water interacts with immersed surfaces, altering the electrokinetic behaviour of small particles, and in general, dominating subsequent surface chemical behaviour. The remarkable property of this surface active material is its non-selective attachment to solids of widely differing composition and surface polarities. Some very recent Russian results (in press) suggest that the surface active material is a liquid phase colloid transported to surfaces by diffusion or convective diffusion. Surface films of the type suggested by these studies provide much greater thicknesses than the molecular lengths of normal collectors or tensides.

Because sea water has such a dramatic effect on the surface properties of introduced particles and bubbles, the first phase, Phase I, of our proposed experimental plan is designed to examine the effect of sea water immersion on the surface character of bubbles and particles of various kinds, both in the absence and in the presence of added surface modifiers.

This will be followed by Phase II which will attempt to define what characteristics of a particle are important if one is to maximize bubble-particle interaction. Parameters to be considered here will be particle composition, shape and surface roughness.

The final part of this study will be Phase III and will test particle collection efficiencies using bench-scale experiments to simulate both the quiesent and turbulent conditions commonly encountered at sea. Collection efficiencies for particles of various compositions and surface characteristics will be determined when using bubbles with a range of sizes and in sea water both in its natural state and with added collectors.

Experiments will also be conducted with sea water collected from the Northwest Arm of Halifax Harbour during different times of the year in order to ascertain the effect on particle collection efficiency of the qualitative and quantitative changes that occur in the organic chemical composition of the water due to the annual cycle in biological activity.

The particle bubble systems which show the most favourable collection efficiencies will then be scaled up and tested by experiments conducted in the Tower Tank. These experiments should be a realistic simulation of the behaviour expected of the systems in the field.

5.2 Phase Ia: Baseline studies

Two kinds of measurements will be used to follow changes in the character of surfaces immersed in sea water. The first involves determination of electrophoretic mobilities of small bubbles and particles as a function of time of exposure to samples of natural sea water. We will use the techniques that we have developed for generating small bubbles and also for handling and aging small bubbles (e.g. Johnson et al. 1982, Johnson and Cooke 1980). In cases where stable microbubbles are generated, we will determine bubble electrophoretic mobilities to sizes as small as 5μm in radius. For bubbles that are not stable, mobilities will be determined to sizes as small as that at which LaPlace pressure produces rapid dissolution, i.e. of the order of 25 μm in radius. Electrophoretic mobilities of larger bubbles as a function of aging time in sea water will be determined in a rotating cell of the type described by Dibbs (1974).

The kinetics of particle surface alteration by natural surfactants will be studied with particles of a wide range of surface properties, e.g. SiO_2- an acidic oxide, Al_2O_3 - a basic oxide, XAD-2 - a hydrophobic polymer, and other particles with various surface characteristics. Aging of particles will be performed in sufficiently large volumes of sea water to ensure that acquisition of the surface film is not limited by the amount of surface active material in the sea water sample. Control experiments will be performed in ultraviolet photo-oxidized sea water or photo-oxidized artificial sea water.

Electrophoretic mobilities of bubbles and particles will be determined with time of aging using a wide range of sea water samples. These samples include coastal samples collected periodically over a year, open ocean surface samples, and samples from phytoplankton cultures.

The second measurement for characterizing acquisition of natural surface films is that of gas-liquid-solid contact angle. We will perform contact angle measurements on the same materials as those used in the electrophoretic mobility studies described above. Similarly aging studies will be conducted to determine the rate of surface alteration by natural surfactants as well as the maximum effect of such alteration as evidenced by the change in contact angle. The results will include advancing and receding contact angle measurements on surfaces with controlled roughness.

While measurements of electrophoretic mobility and contact angle provide sensitive means for following the acquisition of surface films by bubbles and particles in natural sea water, they also provide more fundamental information. For example, Fukui and Yuu (1980) found that particle flotation correlated strongly with the product of zeta potentials. The more negative the product, the more effective flotation. Further, the contact angle has been found to provide important information about the critical film thickness (Schulze 1984).

5.3 Phase Ib: Effect of surface modifiers

Following the baseline studies with particles and bubbles in natural sea water, we will determine the effect of adding particle and bubble surface modifiers (i.e. collectors or tensides), on elecrophoretic mobilities and contact angles. We will then determine the effect of natural aging in sea water to determine if the bubbles and particles, so treated with collector, retain their modified surface properties.

We will test a wide range of concentrations and types of surface modifiers to determine an additive or additives that give electrophoretic mobilities and contact angles offering maximum theoretical bubble-particle attachment conditions. These results with feedback provided by results of

experiments in phases II and III (described below) will help guide our choice of particle and collector.

5.4 Phase IIa: Determination of particle shape and surface character

During this phase of the study, we will investigate the effects of particle shape and surface character, including adsorbed collector and surface roughness, on the efficiency of bubble-particle attachment. A modified version of the stroboscopic system used by Flint and Howarth (1971) will be used. While they employed a large fixed particle and examined collisions of small particles either settling through the water column or entrained in fluid flow, others have used fixed bubbles in much the same configuration. Since we are interested in collisions of small bubbles with relatively larger particles, we will examine collision and attachment efficiencies using a fixed particle with bubbles released from below. Water will also be introduced from below and will flow upward. The bubble trajectories will be mapped stroboscopically as in the experiment of Flint and Howarth (1971).

Guided by the results of experiments from phase I, we will use a sphere of standard size and establish the optimum combinations of particle composition and collector type and concentration. Because some small particle shapes can only be obtained with specific compositions, i.e. limited by commercial availability or our ability to produce that shape, each new composition of particle will be tested to determine an optimum collector. For example, we have had considerable success in floating particles of SiO_2 that have been silanized. However, silanizing involves the reaction of various silyl compounds with terminal -OH groups on the solid surface and is thus specific for certain solid compositions.

Having established the optimum surface chemical character for particles, we will investigate collection efficiencies of bubbles with particles of specific shapes. Bubble collision and attachment will be investigated for the range of bubble sizes from 5 - 500 μm (where not limited by excessive LaPlace pressures). While we will continue to develop a wide range of particle shapes that will be tested for bubble collection efficiencies, some that we envisage now include:

- Sphere: Almost invariably, studies of particle-bubble collisions have been conducted with spheres as model particles. Theoretical models in which collision efficiencies are treated, likewise involve spheres. While spheres certainly do not represent an optimum shape for collision or attachment, they do provide a basis for comparison of our results to literature values.

- Porous floc: Many studies have treated flotation of small particles with flotation enhanced by the presence of metal hydroxide flocs, e.g. alum. These flocs mechanically trap bubbles and greatly enhance flotation rates. However, floc fragility has been cited in a number of studies as a cause of reduced flotation rate in turbulence or in the presence of larger bubbles and this problem may have to be addressed. A great advantage to the use of hydroxide flocs is the ease by which they could be generated in-situ in the ocean by the addition of strong base to sea water. In addition, the material would automatically dissipate when the pH of the area returned to normal levels.

- Rod-shaped: These would be tested with different aspect ratios. Also, since collection of bubbles by rod-shaped particles is undoubtedly orientation-specific, we will investigate the effects of angular orientation on bubble collection.

- Spined sphere: A sphere with spines that are long compared with the radius of the sphere is a 3-dimensional analog of rod shaped particles in various angular attitudes. While a method of production of such particles is not obvious to us at present, this shape may offer high collection efficiencies. It is of interest to note that many species of marine diatoms have just such a shape which presumably has evolved to confer some fluid dynamic advantage. The fact that this shape exists in nature also suggests that they might be cultured and/or harvested for experimental purpose

Particle handling: We have experienced several problems in the production and handling of particles with nonpolar surfaces (e.g. silanized quartz). These hydrophobic particles cannot be removed from water and easily reintroduced in dry form. They merely floculate at the interface. In handling these particles we have used several methods effectivly. We have had some success in introducing hydrohobic particles to water by first suspending them in ethanol. The best approach, however, seems to be to leave them suspended in distilled, deionized and degassed water. Small concentrations (ca. 0.1%) of surfactant (e.g. Triton 100), can usually provide enhanced stability. When this slurry is added to water, the surfactant rapidly diffuses away.

5.5 Phase IIb: Effect of surface roughness on bubble attachment

Particulate surface roughness is a variable that has been found important in rupture of thin films. Rougher particle surfaces puncture films and promote rapid hole formation with attendant three phase contact. When particle shape and collector concentration have been chosen for optimal bubble collection for a given particle, we will test the effect of enhanced surface roughness on bubble-particle collection efficiencies. Surface roughness also affects the strength of bubble-surface attachment and may be a factor in enhancing flotation rates in turbulence.

5.6 Phase IIIa: Bench-scale flotation experiments

In the stroboscopic experiments, bubble-particle collisions occur by sedimentation (bubble rise in our case) and interception. However, in natural systems where turbulence prevails, particle-bubble collisions may be dominated by inertial effects. In addition, turbulence induces bubble-particle aggregate breakup. Thus, in this series of experiments, we will investigate bubble-particle interaction under both quiescent and turbulent conditions.

Bubbles will be produced in sea water in controlled, narrow size ranges between 5-500 μm in radius using the bubble generators described in section 4. Bubble size will be established by shear rate and numbers

produced controlled by gas flow rate. Bubbling will proceed until an obvious steady state of bubble input and bubble breaking has been established. Particles with specific shape, surface roughness, and collector type and concentration will be injected in controlled number to a predetermined depth in the bubbling chamber. Particles that are floated will be collected by microlayer filtration. The progress of flotation, i.e. the numbers of particles floated as a function of time, will be determined either by examination of the microlayer filter or by shadowgraph of the particles remaining in the column. The second method involves exposure of sheet film by a flash of collimated light passing through the bubble chamber. Shadow images of particles and bubbles appear on the film. This method is particularly effective at low bubble and particle concentrations and for larger particle sizes. Flotation rates for particles of different shapes and surface treatments (scaled for differences in mass), will provide a measure of relative particle effectivness for bubble flotation.

The experiments described as phase IIIa will be repeated under conditions with various intensities of turbulence. This will provide a means of assessing the combined effects of inertial impaction and disaggregation for bubbles of different sizes with particles of differing characteristics, i.e., shape and surface character. The rate of energy dissipation, ϵ, can be determined from the rate of energy input via an impeller. The necessity of including baffles in the bubble chamber will be determined through experience with the system.

5.7 Phase IIIb: Large scale flotation experiments

The Aquatron facility at Dalhousie offers a unique opportunity to extend the batch mode tests that have been described in section 5.6. The results of the bench-scale experiments will be further tested in the Tower Tank of the Aquatron facility (for specifications see Appendix A). Large populations of bubbles will be generated using scaled-up versions of our laboratory bubble generators and will be introduced in the centre of the tank and at about 2 meters depth. Above the bubble source will be located an impeller forcing water downward and dispersing the small bubbles. This impeller will only be required to provide organized motion and will not

induce cavitation. The flow that will result is torroidal, and should have a vertical dimension of the order of one half the diameter of the tank (ca. 3 m dia.). The flow will be direct downward in the centre and upward along the wall of the tank.
When a steady state population is achieved, after bubbling for a time long in comparison to the characteristic time of the torroidal circulation, the gas flow will be stopped (circulation via impeller will continue).

The decay of particle-treated and control bubble populations thus generated will be followed using acoustic and photographic methods. The optimized particles and collector will be added to the treatment populations at t=0 (when bubble input is stopped) in the form of a slurry. The threshold concentration required to produce increased decay rates in the bubble population will be determined along with the concentration that appears to saturate all available bubble surfaces.

The acoustic system that we will use to follow bubble populations was designed to study sediment transport (Mesotech Systems Ltd.). This instrument produces a short duration, high frequency pulse transmitted in a narrow conical beam. The back scattered signal is gated so that only that signal from a small volume of water is processed. Two transducers will be used: one will operate at a frequency of about 100 KHz (corresponding to the resonance frequency of 30 μm bubbles) and the other at a yet to be determined lower frequency. Both transducers will be located below the torroidal flow cell looking up at the base of the bubble field, and thus reducing signal attenuation from intervening bubbles.

We will calibrate the acoustic device using well-defined bubble populations produced with our laboratory scale bubble generator. Ground truthing will be done by means of photography, using a bubble camera of the type we have used successfully to determine bubble populations at sea (Johnson and Cooke 1979). Once the characteristic bubble decay patterns have been determined photographically, we should thereafter be able to predict the shape of the decay curve form the acoustic measurements. This approach will permit many more experiments to be run than would be possible if exclusively using the somewhat labour intensive photographic method.

6.0 PROJECT BUDGET

6.1 Labour (year 1)

			$ (CDN)	$ (US)
Sr. Res. Scientist	260d	@ 161.54/d	42,000.40	
Research Scientist	260d	@ 153.85/d	40,001.00	
Post Doctoral Fellow	130d	@ 115.38/d	14,999.40	
Technician	260d	@ 96.15/d	24,999.00	
Support Staff	20d	@ 46.15/d	923.00	
Subtotal			**122,922.80**	**(93,123.33)**
Graduate students (3)	780d	@ 33.46/d	26,098.80	(19,771.82)
Benefits	122,922.80 x	0.122	14,996.58	(11,361.05)
Overhead	122,922.80 x	0.384	47,202.36	(35,759.36)

Labour (year 2)

Sr. Res. Scientist	260d	@ 161.54/d	42,000.40	
Research Scientist	260d	@ 153.85/d	40,001.00	
Post Doctoral Fellow	130d	@ 115.38/d	14,999.40	
Technician	260d	@ 96.15/d	24,999.00	
Support Staff	30d	@ 46.15/d	1,384.50	
Subtotal			**123,384.30**	**(93,472.95)**
Graduate students (3)	780d	@ 33.46/d	26,098.80	(19,771.82)
Benefits	123,384.30 x	0.122	15,052.88	(11,403.70)
Overhead	123,384.30 x	0.384	47,379.57	(35,893.61)

6.2 Direct Charges (years 1 & 2)

Materials & Supplies			30,000.00	
Equipment purchase/rental			20,000.00	
Tower Tank Rental	18wk	@ 980.00/wk	17,640.00	
Wet lab space rental	24mo	@ 560.00/mo	13,440.00	
Travel			12,000.00	
Publication expenses			10,000.00	
Telephone, telex			900.00	
Copying			800.00	
Subtotal			**104,780.00**	**(79,378.79)**
TOTAL COST			527,916.09	(399,936.43)

6.3 Certification

This proposal is approved under the general policy of Dalhousie University regarding research contracts.

Chairman, Department of Oceanography

Vice Pres., Academic

7.0 REFERENCES

Acrivos, A. and J.D. Goddard (1965) J. Fluid Mech. 23: 273.

Ahmed, N. and G.J. Jameson (1985) Int. J. Miner. Process. 14: 195.

Anfruns, J.F. and Kitchener, I.A. (1977) Bull. Inst. Min. & Metallurgy Trans. Sect. C 86: 9.

Baccuber, C. and C. Sanford (1974) J. Appl. Phys. 45: 2567.

Blake, T.D. and J.A. Kitchener (1972) J. Chem. Soc. Faraday Trans. 68: 1435.

Cassell, E.A., K.M. Kaufman and E. Matjevic (1974) Water Res. 9: 1017.

Clift, R., J.R. Grace and M.E. Weber (1978) Bubbles Drops and Particles, Academic Press, New York, 380pp.

Clint, D.H. and T. Walker (1974) J. Colloid Int. Sci. 77: 172.

Collins G.L. and G.J. Jameson (1976) Chem. Eng. Sci. 31: 985.

Devivo, D.G. and B.L. Karger (1970) Sep. Sci 5: 145.

Dibbs, H.P., L.L. Sirois and R. Bredin (1974) Can. Metall. Quart. 13: 395.

Flint, L.R. and W.I. Howarth (1971) Chem. Eng. Sci. 26: 1155.

Fuks, N.A. (1977) Mechanika aerozolej., Izdat. Akad. Nauk SSSR, Moscow.

Fukui, Y. and S. Yuu (1980) Chem Eng. Sci. 35: 1097.

Gaudin, A.M. (1957) Flotation, 2nd edition, McGraw Hill, New York, p. 147.

Gershey, R.M. (1983) Limnol. Oceanogr. 28: 309.

Gershey, R.M. (1983) Limnol. Oceanogr. 28: 395.

Hunter, K.A. (1980) Limnol. Oceanogr. 25: 807.

Johnson, B.D., R.M. Gershey, R.C. Cooke and W. Suttcliffe (1982b) Limnol. Oceanogr. 27: 369.

Johnson, B.D. and R.C. Cooke (1981) Science 213: 209.

Johnson, B.D. and R.C. Cooke (1980) Limnol. Oceanogr. 25: 653.

Johnson, B.D., R.M. Gershey, R.C. Cooke and W. Suttcliffe (1982a) Separation Science 17: 1027.

Johnson, B.D. and R.C. Cooke (1979) J. Geophys. Res. 84: 3761.

Johnson, B.D. (1981) Limnol. Oceanogr. 26: 992.

Kitchener, J.A. (1975) Chem. & Ind. 2: 54.

Langmuir (1942)

Levich, V.G. (1962) Physicochemical Hydrodynamics, Prentice Hall, Englewood Cliffs, N.J.

Mangravite, F.J. Jr., E.A. Cassel and E. Matijevic (1972) J. Coll. Inter. Sci. 39: 357.

Medwin, H. (1977) J. Geophys. Res. 82: 971.

Morris, T.M. (1950) Amer. Inst. Metallurg. Eng. Trans. 187: 91.

Mulhearn. P.J. (1981) J. Geophys. Res. 86: 6429.

Natarajan, R., et.al. (1983) Sci. Technol. Miner. Benif. India. Proc. Symp. 1981, pp. 197.

Niehoff, R. and G. Loeb (1972) J. Mar. Res. 32: 5.

Ninham, B.W. and V.A. Parsegian (1970) J. Chem. Phys. 52: 4578.

Reay, D. and G.A. Ratcliffe (1973) Can J. Chem. Eng. 51: 178.

Reay, D. and G.A. Ratcliffe (1975) Can J. Chem. Eng. 53: 481.

Rubin, A.J. and S.F. Erickson (1971) Wat. Res. 5: 437.

Schulze, H.J. (1984) Physico-chemical Elementary Processes in Flotation, Elsevier, New York.

Schulze, H.J. (1975) Colloid Polymer Sci. 253: 730.

Sutherland, K.L. (1948) J. Phys. Chem. 52: 394.

Tomlinson, H.S. and M.G. Fleming (1963) Flotation rate studies. 6th Intl. Mineral Processing Congress, Cannes, Pergamon Press, p. 563.

Wallace, G.T. Jr. and R.A. Duce (1975) Marine Chem. 3: 157.

Weber, M.E., D.C. Blanchard and L.D. Syzdek (1983)

Wilson, D.J. and R.M. Kennedy (1979) Sep. Sci. Tech. 14: 319.

8.0 NOTATION

a	particle radius	(L)
A	bubble radius	(L)
A_p	projected bubble area	(L^2)
D	diameter of frit pore	(L)
d	bubble diameter	(L)
D_f	diffusivity	(L^2/T)
d_p	particle diameter	(L)
F_D	drag force	(F)
G	pressure gradient	(F/L^2)
h_{crit}	critical film thickness	(L)
K	mass transfer coefficient	(L/T)
L	distance from frit centre	(L)
L_w	radius of circular frit	(L)
R	radius of bubble	(L)
r_1	diameter of sleeve	(L)
r_2	diameter of cylindrical frit	(L)
R_B	radius of bubble	(L)
R_M	distance to bubble axis	(L)
R_p	radius of particle	(L)
S	channel width	(L)
U	local velocity	(L/T)
U_∞	velocity at large distance	(L/T)
U_{avg}	average velocity	(L/T)
U_o	fluid velocity	(L/T)
U_{rel}	relative velocity	(L/T)
U_{vol}	volume flow rate	(L^3/T)
V	rise velocity	(L/T)
W	gas flow rate	(L^3/T)
y	distance from plane surface	(L)
f	fluid density	(FT^2/L^4)
ϵ	energy dissapation	(L^2/T^3)
Γ	gas-water surface tension	(F/L)
π	disjoining pressure	(F/L^2)
μ	dynamic viscosity	(FT/L^2)
τ	sliding time	(T)
Φ	stream function	
ϕ	critical angle	

DIMENSIONLESS PARAMETERS

C_D	drag constant
E	collision efficiency
E_i	collision efficiency (interception)
G_p	gravity parameter
N	number of bubbles
Pe	Peclet number
Re	Reynolds number
Sc	Schmidt number
Sh	Sherwood number
St	Stokes number

APPENDIX A

Aquatron faciility, Dalhousie University

Aquatron Laboratory
Dalhousie University
Marine and Freshwater Research Opportunities

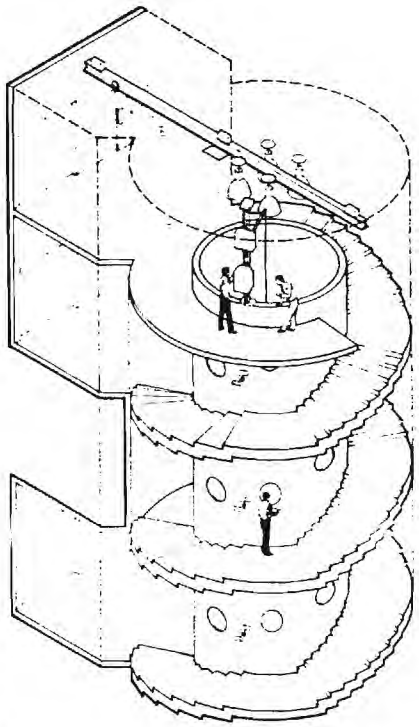

The Aquatron Laboratory offers large-scale and specialized research facilities for use by scientists and engineers involved in the study of marine or freshwater systems. Integrated within the Life Sciences Centre on the Dalhousie University campus, the facility is serviced by flowing filtered seawater and dechlorinated freshwater.

Pool Tank: Cylindrical aquarium tank, 15.2 m diameter, 3.7 m deep, volume 685 m^3. Temperature and/or salinity can be controlled in static or flow-through modes. An axially suspended rotating bridge provides access over the tank and can be used for towing equipment. Overhead mercury lights provide controlled light cycles, and 22 underwater viewing windows provide excellent observational capabilities. *Research Programs:* Behaviour, ecology and energetics of fish, cephalopod and zooplankton schools, as well as of larger marine animals such as seals and sharks; Aquaculture physiology and technology; Equipment development and testing.

Tower Tank: Silo-shaped tank, 10.5 m deep, 3.7 m diameter, volume 117 m^3. Water column can be stratified with respect to both temperature and salinity. Light regime in the tank can be controlled with timers on 6 overhead metal halide lamps. Access to 26 viewing ports is by a helical stairway. Winches allow deploying equipment weighing up to one ton. A flexible plastic divider can be deployed in the tank to provide experimental duplication or control. *Research Programs:* Mesocosm research with planktonic communities; Plankton vertical migration; Salmon aquaculture physiology and technology; Cephalopod spawning and larval ecology; Equipment development and testing.

Seal Tank: Outdoor tank, designed for research on seals. Volume 50 m^3, dimensions 6.5 m x 3 m x 2 m deep. Large deck surrounds the tank at water level and an enclosed lab overhangs one end of the tank. *Research Programs:* Seal behaviour and parasitology.

Seawater Flume Tank: 3.2 m flume with controlled flow rates up to 30 cm s^{-1}. *Research Programs:* Benthic boundary-layer processes involving particle flux, sediment stability, and feeding interactions.

Swim Tunnel Respirometer: Recirculating swim tunnel with inner diameter of 19.2 cm, salinity and temperature control, and capable of velocities up to 2 m s^{-1}. *Research Programs:* Energetics and physiology of fish and cephalopods.

Experimental Aquarium Rooms: Ten sets of paired wet and dry labs have individual control of water temperature and salinity, in open or recirculation modes. *Research Programs:* Phytoplankton mass culturing; Zooplankton feeding and behaviour; Lobster culture; Sea urchin disease; Cold water crab physiology; Aquacultural genetics; Age determination of molluscs.

Program Time: The Aquatron Laboratory is maintained by Dalhousie University with NSERC support as a marine and freshwater research facility, and is available for use by scientists and engineers from other universities as well as from industrial and government laboratories.

A limited number of visiting research fellowships are available to assist with costs with use of the facility by external researchers. Inquiries for further information and requests for program time or participation in collaborative projects with Dalhousie researchers should be made to **Dr. Norval Balch, Aquatron Laboratory, Dalhousie University, Halifax, Nova Scotia, Canada, B3H 4J1; phone (902) 424-3874; Omnet (DALHOUSIE.OCEAN).**